SAND2005-8029C

Length Scale Effects on Deformation and Failure Mechanisms of Ultra-Fine and Nanograined Metals

K. Hattar[1], J. H. Han[2], D. M. Follstaedt[3], S. J. Hearne[3], T. A. Saif[2], I. M. Robertson[1]
[1]Materials Science and Engineering, University of Illinois,
1304 W. Green St. Urbana, IL 61801 USA
[2]Mechanical and Industrial Engineering, University of Illinois,
1206 W. Green St. Urbana, IL 61801 USA
[3]Physical, Chemical and Nano Sciences Center, Sandia National Laboratories
P. O. Box 5800, MS 1056 Albuqerque, NM 87185

ABSTRACT

The deformation and failure processes in ultra-fine and nanograined metals over different length scales have been probed using transmission electron microscopy (TEM) and scanning electron microscopy (SEM) in combination with a micromechanical *in situ* straining device. This novel straining device affords the opportunity to directly correlate the macroscopic mechanical properties with the microscopic deformation and failure mechanisms. Through use of this device it has been shown that increased film thickness results in a transition between limited plasticity and intergranular fracture to global plasticity and shear failure for deposited aluminum samples of similar grain size but different thickness.

INTRODUCTION

The mechanical properties of nanograined and ultra-fine grained metals exhibit a higher yield and fracture strength, lower elongation and toughness, higher strain rate sensitivity, higher strain rate sensitivity index, lower ($<10b^3$) activation volume, and higher wear resistance than the corresponding large grained counterparts. The stress-strain curves of nanograined materials, as well as ultra-fine grained ones, are characterized by an initial region of rapid strain hardening followed by a flat plastic region with almost no work hardening. That is, the response is almost elastic and perfectly plastic. This lack of strain hardening, which is not compensated for by the increased strain rate sensitivity index, makes these materials prone to inhomogeneous or localized deformation and accounts for the limited ductility. Shear banding or localization has been reported for bcc metals[1,2] but less frequently in fcc metals.[3,4]

Despite extensive molecular dynamics computer simulation[5-15] and experiments,[16] including *in situ* TEM deformation studies,[17-21] there is still debate over the deformation mechanisms and processes responsible for the observed macroscopic response. It has been proposed that the deformation mechanism changes from dislocation mediated to grain-boundary processes as the grain size decreases. Within the dislocation mediated response there is further division, with perfect dislocations dominating at large-grain sizes, and partial dislocations and then deformation twins dominating at smaller and smaller grain sizes. Clear demarcation of the transition grain sizes has not been established and there is some debate about the existence of such well-defined transitions.

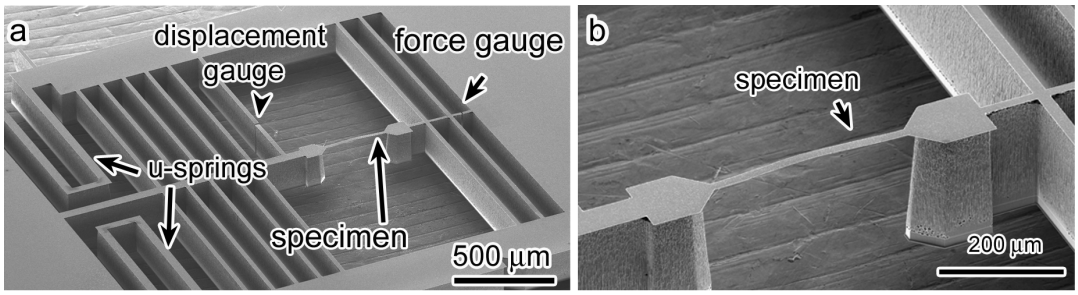

Figure 1. a) Straining device and b) magnified image of free-standing metallic film.

In this paper, we report on *in situ* TEM deformation studies of free-standing thin metallic films with a columnar ultra-fine grain structure.

EXPERIMENTAL PROCEDURE

A novel microfabricated device shown in Figure 1, was used to relate the controlling deformation and fracture mechanisms and mechanical properties of ultra-fine grained, free-standing aluminum thin films; details on the fabrication process can be found in ref.[22,23] The device provides the capability for straining within the confines of the TEM under uniaxial loading. The stress and strain can be directly determined during *in situ* experiments from measurement of the relative displacement of the force and strain gauges indicated in Figure 1. Straining of the device was achieved by means of a conventional TEM straining stage operated in a displacement controlled mode. Al films 125 and 500 nm thick were deposited on the Si wafer prior to fabrication by either sputter deposition (125 nm thick film) or electron beam evaporation (500 nm film). The dimensions of the gauge sections were either 300 x100 x 0.125 µm or 180 x 30 x 0.500 µm. *In situ* TEM straining experiments were conducted using a JEOL 4000 and a Philips CM12 TEM operating at 300 kV and 120 kV, respectfully.

RESULTS

All films had a columnar grained structure with no dislocations, second phases, or voids evident in the grains or grain boundaries, see Figure 2. The grain size distributions for the 125 nm sputter deposited film and the 500 nm e-beam evaporated films are compared in Figure 2c. Both films exhibit a wide grain size distribution with average sizes of 120 nm and 130 nm for the e-beam and sputtered films, respectfully.

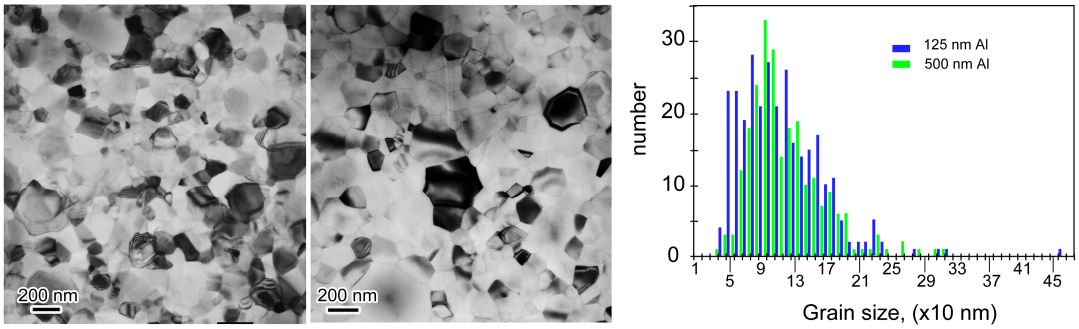

Figure 2. a) Initial microstructure for 125 nm sputter deposited film b) Initial microstructure for 500 nm sputter deposited film c) Comparison of grain size distributions.

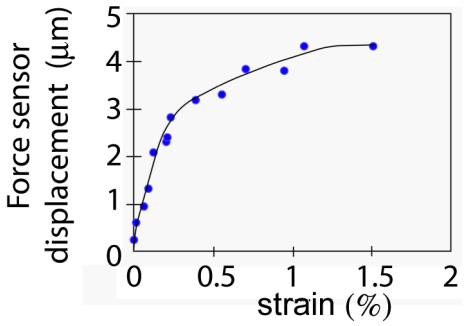

Figure 3. Mechanical response of a 500 nm thick Al film. Sample had not failed at 1.5 % strain.

Measurements of the macroscopic properties of the 500 nm thick film show the same behavior as other nanograined systems, decreased ductility, and reduced strain hardening after a short period of high strain hardening, see Figure 3. Note in Figure 3, the ordinate is not given as stress as the spring constant for the force sensor gauge was not determined. Nevertheless, the curve displays the characteristics of bulk deformed ultra-fine and nanograined materials. Observations during *in situ* TEM straining experiments relate the motion of bend contours to the region of elastic behavior and the combined motion of dislocations and bend contours to the plastic region. All dislocations observed moved unhindered across grains from one grain boundary to the opposite one; for examples, see micrographs in figure 4.[23] In contrast in the thinner films, there was no evidence of general dislocation activity, although there was evidence of bend contour activity throughout the gage section.

The failure mechanism was found to also depend on the sample thickness. In the 125 nm thick film, the failure crack propagated rapidly through the grain boundaries with limited evidence for plasticity. Dislocation activity occurred only in larger grains that had halted the advancing crack.[22] The dislocation activity was confined to the one large grain in which dislocation pile-ups formed. This resulted in crack blunting that was very effective in arresting the crack to the extent that another crack nucleated and propagated elsewhere. The failure surface was normal to the tensile axis. SEM examination of fracture surface was consistent with intergranular failure. Examples showing this failure behavior are presented in Figure 5.

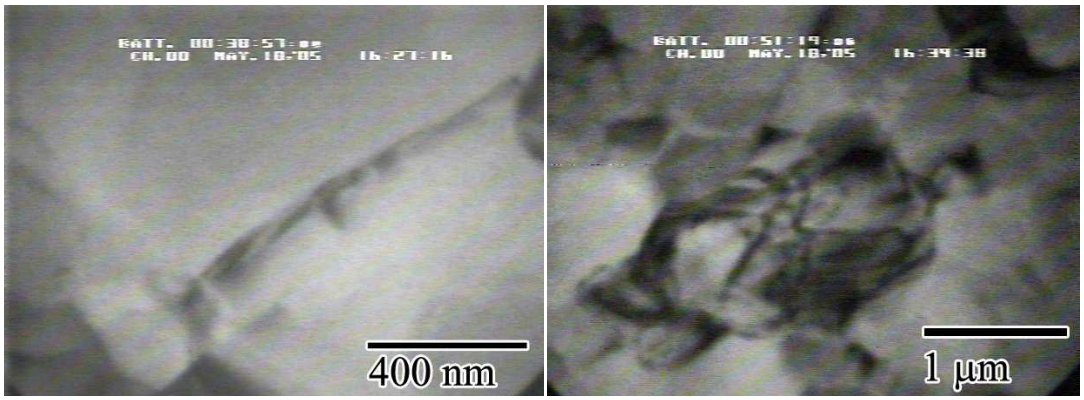

Figure 4. Dislocation activity a) in the grain boundary and b) in the grain interior.

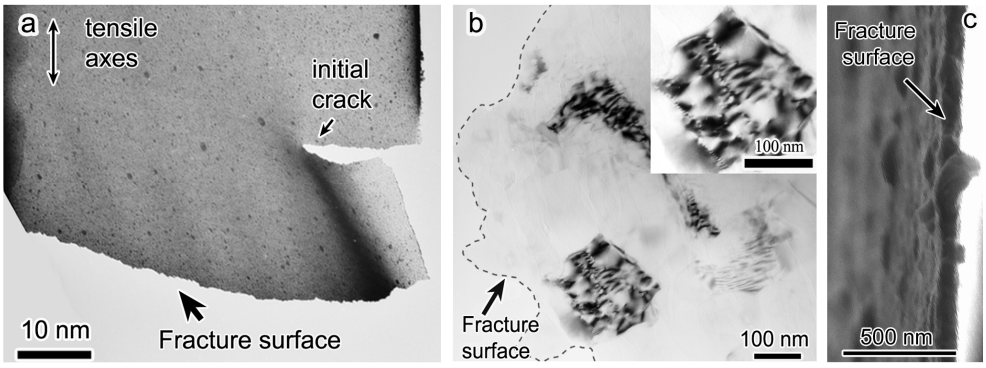

Figure 5. a) Fracture surface, b) dislocations in grains along the fracture surface and SEM micrograph of the fracture surface of the 125 nm thick film.

In contrast to the thinner sample, the 500nm thick film exhibited a shear failure with the fracture surface at 30° to the tensile axis. The shear band extended 300 to 400 nm from the fracture surface and all grains contained dislocations with dislocation arrays forming in some of the larger grains, see Figure 6b. Examination of the fracture surface revealed that the grains along the fracture surface had undergone extensive thinning resulting in a knife-edge failure, which is consistent with extensive local plasticity, Figure 6c. A similar shear fracture was observed for a 200 nm thick gold sample with an average grain size of 80 nm. In that case, the shear band extended 200 to 500 nm from the fracture surface which ran at a 45° angle to the tensile axis.[24] This shear band failure is anticipated in materials with limited or no strain hardening ability, as is the observed limited ductility.

DISCUSSION

A different deformation and failure response has been found for Al films of different thicknesses. The two films considered were grown by different processes; the thinner film was produced by sputter deposition and the thicker film by electron beam evaporation. Both films have similar grain size distributions and similar average grain sizes, eliminating this as a possible cause for the different behavior. Another possibility is that the composition of the films is

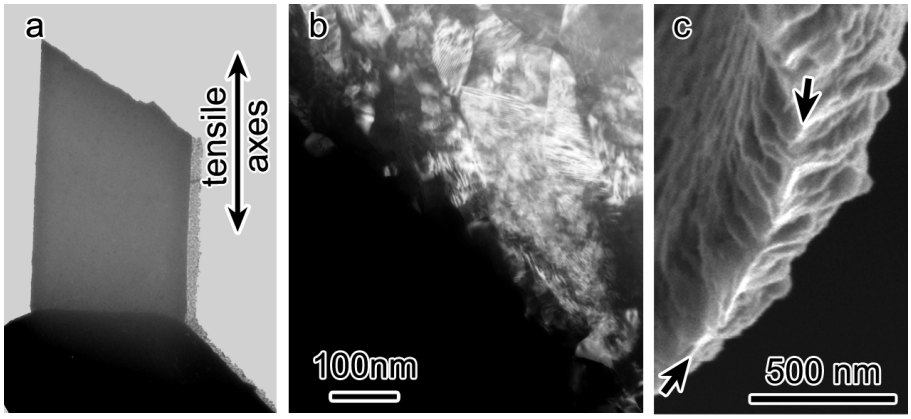

Figure 6. a) Fracture surface, b) dislocations in grains along the fracture surface and SEM micrograph of the fracture surface of the 500 nm thick film.

different. To determine the composition and the level of impurities several techniques were employed. Energy dispersive x-ray analysis showed no second phase or chemical contamination in the films. Electron energy loss analysis detected slightly larger (2 at%) concentration of oxygen at the grain boundaries in the thinner sputter deposited samples, but this difference may be a consequence of sample roughness. Rutherford backscattering analysis also found less than one atomic percent contamination. However, trace levels of sulfur and argon were detected in the sputter deposited film, which was likely the result of microfabrication and sputter deposition techniques, respectfully. From this chemical analysis, it appears that the difference in failure mechanisms is not due to compositional differences. This conclusion is supported by preliminary work on Al films of varying thicknesses prepared by electron beam evaporation, which show that the response of a 150 nm thick Al film exhibits the same deformation and failure characteristics as the 125 nm thick film produced by sputter deposition.

The different responses in these two film thicknesses raises questions about the viability of conducting *in situ* TEM deformation experiments on nanograined and ultra-fine grained metallic films. For the observed mechanisms to be applicable to bulk materials it is essential that the same conditions prevail for both samples, which as demonstrated is not the case for the 125 nm thick Al film. Further work is in progress to determine the threshold thickness for this transition as well as the effects of grain size, grain size distribution, temperature, and the addition of solute on the deformation and failure mechanisms of the system.

CONCLUSION

Deformation and failure mechanisms for ultra-fine columnar grained aluminum films were investigated using a combination *in situ* TEM and SEM techniques that allowed for a direct relation between the governing mechanisms and mechanical properties to be formulated. It was determined that 125 nm sputter deposited aluminum films failed intergranularly perpendicular to the strain axis with limited plasticity along the fracture surface. In contrast, 500 nm thick samples produced by electron beam deposition exhibited shear-band failure with extensive dislocation activity evident in the shear band and knife-edge. This study determined that film thickness plays an important role in the deformation and failure mechanisms of ultra-fine grained metal films.

ACKNOWLEDGEMENTS

This research was supported by a grant from NSF DMR, award # 02037400. The electron microscopy was performed in the Center for Microanalysis of Materials, University of Illinois at Urbana-Champaign, which is partially supported by the U.S. Department of Energy under grant DEFG02-91-ER45439 and by the University of Illinois. Sandia is a multiprogram laboratory operated by Sandia Corporation, a Lockheed Martin Company, for the United States Department of Energy's National Nuclear Security Administration under Contract No. DE-AC04-94-AL-85000. This work supported by the Office of Basic Energy Sciences, and done under the auspices of the Center of Integrated Nano Technologies.

REFERENCES

1 Q. Wei, S. Cheng, K. T. Ramesh, and E. Ma, Mater. Sci. & Engin. A **381,** 71 (2004).

2 D. Jia, K. T. Ramesh, and E. Ma, Acta Materialia **51,** 3495 (2003).

3 F. D. Torre, H. V. Swygenhoven, and M. Victoria, Acta Materialia **50,** 3957–3970 (2002).

4 S. Cheng, E. Ma, Y. M. Wang, L. J. Kecskes, K. M. Youssef, C. C. Koch, U. P. Trociewitz, and K. Han, Acta Materialia **53,** 1521 (2005).

5 D. Wolf, V. Yamakov, S. R. Phillpot, A. Mukherjee, and H. Gleiter, Acta Materialia **53,** 1 (2005).

6 V. Yamakov, D. Wolf, S. R. Phillpot, and H. Gleiter, Acta Materialia **50,** 61 (2002).

7 H. Van Swygenhoven, F. Dalla Torre, and M. Victoria, Acta Materialia **50,** 3957 (2002).

8 H. Van Swygenhoven and P. M. Derlet, in *What simulations suggest on deformation mechanism in Nc-metals*, Ultrafine Grained Materials III Charlotte, NC., United States, 2004 (Minerals, Metals and Materials Society, Warrendale, United States), p. 11-16.

9 H. Van Swygenhoven, P. M. Derlet, and A. Hasnaoui, Physical Review B **66,** 24101 (2002).

10 H. Van Swygenhoven, P. M. Derlet, and A. Hasnaoui, Advanced Engin. Mater. **5,** 345 (2003).

11 H. Van Swygenhoven, M. Spaczer, and A. Caro, Acta Materialia **47,** 3117 (1999).

12 V. Yamakov, D. Wolf, S. R. Phillpot, and H. Gleiter, Acta Materialia **50,** 5005 (2002).

13 V. Yamakov, D. Wolf, S. R. Phillpot, and H. Gleiter, Acta Materialia **51,** 4135 (2003).

14 J. Schiotz, Mater. Sci. and Engin. A **375-377,** 975 (2004).

15 J. B. Bilde-Sorensen and J. Schiotz, Science **300,** 1244 (2003).

16 Y. M. Wang, A. V. Hamza, and E. Ma, Applied Physics Letters **86,** 241917 (2005).

17 K. S. Kumar, S. Suresh, M. F. Chisholm, J. A. Horton, and P. Wang, Acta Materialia **51,** 387-405 (2003).

18 K. Jagannadham, H. G. F. Wilsdorf, and J. Weertman, Materials Research Innovations **1,** 254 (1998).

19 R. Mitra, W.-A. Chiou, and J. R. Weertman, J. Materials Research **19,** 1029-1037 (2004).

20 R. C. Hugo, H. Kung, J. R. Weertman, R. Mitra, J. A. Knapp, and D. M. Follstaedt, Acta Materialia **51,** 1937-1943 (2003).

21 Z. Shan, E. A. Stach, J. M. K. Wiezorek, J. A. Knapp, D. M. Follstaedt, and S. X. Mao, Science **305,** 654 (2004).

22 K. Hattar, J. Han, M. T. A. Saif, and I. M. Robertson, J. Materials Research **20,** 1869 - 1877 (2005).

23 K. Hattar and I. M. Robertson, unpublished work, (2005).

24 K. Hattar, J. Han, T. Saif, and I. M. Robertson, in *Development and Application of a MEMS-Based In Situ TEM Straining Device for Ultra-Fine Grained Metallic Systems*, Microscopy and Microanlysis Society, 2004.